Available online at www.sciencedirect.com
ScienceDirect
Journal of Nutritional Biochemistry 19 (2008) 216–228
Journal of Nutritional Biochemistry

RESEARCH ARTICLES

Loss of PPARγ in immune cells impairs the ability of abscisic acid to improve insulin sensitivity by suppressing monocyte chemoattractant protein-1 expression and macrophage infiltration into white adipose tissue

Amir J. Guri[a], Raquel Hontecillas[a], Gerardo Ferrer[a], Oriol Casagran[a], Umesh Wankhade[a], Alexis M. Noble[a], Decio L. Eizirik[b], Fernanda Ortis[b], Miriam Cnop[b], Dongmin Liu[a], Hongwei Si[a], Josep Bassaganya-Riera[a,*]

[a]*Laboratory of Nutritional Immunology and Molecular Nutrition, Virginia Polytechnic Institute and State University, Blacksburg, VA 24061, USA*
[b]*Laboratory of Experimental Medicine, Université Libre de Bruxelles, B-1070 Brussels, Belgium*

Received 17 November 2006; received in revised form 6 February 2007; accepted 14 February 2007

Abstract

Abscisic acid (ABA) is a natural phytohormone and peroxisome proliferator-activated receptor γ (PPARγ) agonist that significantly improves insulin sensitivity in db/db mice. Although it has become clear that obesity is associated with macrophage infiltration into white adipose tissue (WAT), the phenotype of adipose tissue macrophages (ATMs) and the mechanisms by which insulin-sensitizing compounds modulate their infiltration remain unknown. We used a loss-of-function approach to investigate whether ABA ameliorates insulin resistance through a mechanism dependent on immune cell PPARγ. We characterized two phenotypically distinct ATM subsets in db/db mice based on their surface expression of F4/80. F4/80^{hi} ATMs were more abundant and expressed greater concentrations of chemokine receptor (CCR) 2 and CCR5 when compared to F4/80^{lo} ATMs. ABA significantly decreased CCR2^{+} F4/80^{hi} infiltration into WAT and suppressed monocyte chemoattractant protein-1 (MCP-1) expression in WAT and plasma. Furthermore, the deficiency of PPARγ in immune cells, including macrophages, impaired the ability of ABA to suppress the infiltration of F4/80^{hi} ATMs into WAT, to repress WAT MCP-1 expression and to improve glucose tolerance. We provide molecular evidence in vivo demonstrating that ABA improves insulin sensitivity and obesity-related inflammation by inhibiting MCP-1 expression and F4/80^{hi} ATM infiltration through a PPARγ-dependent mechanism.

Keywords: Adipose tissue; Inflammation; Phytochemical; Abscisic acid; Macrophages

1. Introduction

Obesity is characterized by low-grade chronic inflammation and insulin resistance. In parallel with the obesity epidemic, the prevalence of insulin resistance and type 2 diabetes (T2D) has also seen a precipitous growth [1]. Adipocyte hypertrophy is believed to be at the core of the pathogenesis of obesity-induced insulin resistance [2,3]. Hypertrophic adipocytes are insulin resistant and secrete more free fatty acids (FFAs) and triglycerides (TGs) than they take up, leading to lipid deposition in peripheral tissues such as the liver and skeletal muscles; they also produce chemokines, such as monocyte chemoattractant protein-1 (MCP-1) and macrophage inflammatory protein 1α (MIP-1α), which promote macrophage infiltration into white adipose tissue (WAT) [4–6]. Macrophages, not adipocytes, are the main pro-inflammatory mediators in WAT, and these cells play a prominent role in the induction and maintenance of obesity-induced inflammation and insulin resistance [2,5].

Thiazolidinediones (TZDs) are drugs that improve systemic insulin sensitivity mostly by activating the nuclear receptor, peroxisome proliferator-activated receptor γ (PPARγ) [7]. This nuclear receptor is endogenously activated by some polyunsaturated fatty acids and products of lipid metabolism [8]. PPARγ activation significantly attenuates adipocyte hypertrophy and inhibits WAT inflammation [5,9]. The

* Corresponding author. Tel.: +1 540 231 7421; fax: +1 540 231 3916.
E-mail address: jbassaga@vt.edu (J. Bassaganya-Riera).

0955-2863/$ – see front matter © 2008 Elsevier Inc. All rights reserved.
doi:10.1016/j.jnutbio.2007.02.010

prevailing notion is that the beneficial actions of TZDs in the uncoupling of obesity from insulin resistance are mediated by adipocyte PPARγ, which induces the transcription of a number of adipogenic genes and is essential for the differentiation of preadipocytes into adipocytes [8,10,11]. The increased adipocyte differentiation induced by PPARγ ligands significantly increases the number of small insulin-sensitive adipocytes; augments insulin-stimulated glucose, FFA and TG uptake from the circulation; and partitions FFAs away from skeletal muscles and the liver; these effects will result in decreased extra adipose fat deposition [12].

Immune cells, the key pro-inflammatory mediators in the WAT of obese mice and humans, also express PPARγ and are plausible therapeutic targets for PPARγ agonists [13,14]. Thus, it is possible that the clinically proven efficacy of PPARγ agonists in T2D prevention and treatment [15] is also mediated via the anti-inflammatory actions of PPARγ activation in immune cells. At the molecular level, PPARγ is a direct transcriptional repressor of chemokine receptor (CCR) 2, the receptor for MCP-1 [16], which is prominently expressed in immune cells, including macrophages. Moreover, MCP-1 expression and secretion are significantly inhibited in WAT following treatment with synthetic PPARγ ligands [4,5]. Whole-body disruption of either *Ccr2* or *Mcp- 1* genes has recently been shown to ameliorate obesity-induced insulin resistance by dampening the recruitment of macrophages into WAT [17–19]. MCP-1 directly inhibits the insulin signaling pathway and may be involved in the progression of hepatic steatosis, which is a paradigm of insulin resistance states due to preserved lipid storage capacity and enhanced gluconeogenesis in the insulin-resistant liver [18,19].

Despite the impressive and persistent benefits of synthetic PPARγ ligands in improving systemic insulin sensitivity, their side effects, including fluid retention, weight gain and, in some cases, congestive heart failure [20], make them unlikely candidates for insulin resistance prevention. Against this background, our laboratory has recently begun examining the insulin-sensitizing effects of the phytochemical and novel PPARγ agonist, abscisic acid (ABA). Administration of ABA to db/db mice improves glucose tolerance and up-regulates PPARγ and PPARγ-responsive gene expression in WAT without affecting body weight [21]. We also observed a significant suppression in WAT tumor necrosis factor α (TNF-α) mRNA expression and macrophage infiltration in ABA-fed db/db mice [21].

To further characterize these promising findings, the present study aims to dissect the expression of PPARγ-responsive and inflammatory genes by adipocytes versus stromal–vascular cells (SVCs) in WAT. We also phenotypically characterized subsets of adipose tissue macrophages (ATMs) targeted by ABA and determined whether ABA ameliorates insulin resistance and obesity-related inflammation through a mechanism dependent upon immune cell PPARγ. Our data demonstrate that SVCs, not adipocytes, are the main producers of PPARγ-responsive genes and chemokines in WAT. In addition, we provide in vivo molecular evidence suggesting that ABA ameliorates glucose tolerance and obesity-related inflammation by suppressing MCP-1 expression and F4/80^{hi} macrophage infiltration into WAT through a mechanism dependent on immune cell PPARγ.

2. Materials and methods

2.1. Mice and dietary treatments

BKS.Cg^{-}+Lepr^{db}/+Lepr^{db}/OlaHsd(db/db) (PPARγ fl/fl), MMTV-Cre^{+}/PPARγ fl/fl and MMTV-Cre^{-} mice in C57BL/6J background were housed in animal facilities at the Virginia Polytechnic Institute and State University in a room maintained at 22°C, with a 12:12 h light–dark cycle starting from 0600 h. All experimental procedures were approved by the Institutional Animal Care and Use Committee of the Virginia Polytechnic Institute and State University and met or exceeded requirements of the Public Health Service/National Institutes of Health and the Animal Welfare Act.

Db/db mice (n=10) were fed high-fat diets with a previously described ingredient composition [21] containing 0 or 100 mg of racemic ABA (Sigma Aldrich, St. Louis, MO) per kilogram of diet for 36 days. On Day 36, fasted mice (12 h) were sacrificed by CO_2 narcosis, and blood was withdrawn directly from the heart for assessment of fasting glucose levels with an Accu-Chek® Glucometer (Roche, Indianapolis, IN). Plasma was also collected for analysis of MCP-1 protein levels and plasma TGs. Abdominal WAT was then excised to generate single-cell suspensions for flow cytometry. Liver specimens were placed in 10% buffered neutral formalin for histological evaluation. Liver samples were also stored in RNAlater (Ambion, Austin, TX), a commercial solution that inhibits RNases, for RNA isolation and quantitative gene expression analyses.

PPARγ floxed mice expressing the *Cre* transgene (e.g., PPAR-γ fl/fl and MMTV-Cre) underwent premature termination of translation following the loss of the exon 2 of PPARγ due to the enzymatic activity of recombinase on genomic DNA [22,23]. PPARγ fl/fl, MMTV-Cre^{+}/PPARγ fl/fl and MMTV-Cre^{-} littermate mice were fed high-fat diets with or without ABA (100 mg/kg). After 28 weeks, the mice were fasted for 6 h and bled through the caudal vein for assessment of fasting blood glucose (FBG) concentrations using an Accu-Chek® Glucometer (Roche). The mice were then subjected to an intraperitoneal glucose tolerance test (GTT; 2 g/kg body weight), with determination of glucose levels at 15, 30 and 90 min postchallenge. At the 90-min time point, mice were sacrificed by CO_2 narcosis. Abdominal WAT was then excised to generate single-cell suspensions for flow cytometry or placed in a 10% buffered neutral formalin for histological evaluation and stored in RNAlater (Ambion) for RNA isolation and quantitative gene expression analyses.

2.2. WAT digestion

Abdominal WAT was excised, weighed, minced into small <10-mg pieces and placed into digestion media consisting of Dulbecco's modified Eagle's medium (DMEM; Mediatech, Herndon, VA) supplemented with 2.5% HEPES (Mediatech) and 10 mg/ml fatty-acid-free bovine serum albumin (FAB-poor BSA; Sigma), Liberase Blendzyme 3 (0.03 mg/ml; Roche) and DNase I (50 U/ml; Qiagen, Valencia, CA). Samples were incubated in a rotating 37°C water bath for 90 min, filtered through a 250-μm nylon mesh (Sefar America, Inc., Depew, NY) to remove undigested particles and centrifuged at 4°C at 1000×*g* for 10 min. The pellet, consisting of SVCs containing endothelial cells, preadipocytes, macrophages and T cells, was washed with DMEM and centrifuged at 4°C at 1000×*g* for 10 min. Supernatant was discarded, and erythrocytes were lysed by incubating SVCs in 2 ml of erythrocyte lysis buffer for 2 min before stopping the reaction with 9 ml of 1× phosphate-buffered saline (PBS). Cells were then centrifuged again at 4°C at 1000×*g* for 10 min, suspended in 1 ml of 1× PBS and enumerated with a Z1 Single Particle Counter (Beckman Coulter, Fullerton, CA). SVCs were resuspended in FACS buffer (1× PBS, 1% normal goat serum and 0.2% sodium azide) at a concentration of 2×10^6 cells/ml. SVCs not used in resuspensions were centrifuged for 5 min at 10,000×*g*, resuspended in RLT lysis buffer (Qiagen) containing 1% β-mercaptoethanol and immediately frozen at −80°C for RNA isolation and gene expression analyses.

2.3. Flow cytometry

SVCs (2×10^5 cells) were seeded into 96-well plates and centrifuged at 4°C at 1800×*g* for 4 min. The cells were then incubated in the dark at 4°C for 20 min in FcBlock (20 μg/ml; BD Pharmingen) and then for an additional 20 min with fluorochrome-conjugated primary antibodies anti-F4/80-PE-Cy5 (5 μg/ml), anti-CD11b-FITC (2 μg/ml; eBioscience), anti-CCR5-PE or anti-CCR2-PE (R&D Systems, Minneapolis, MN). The specific antibody combinations used were F4/80–CD11b–CCR5 and F4/80–CD11b–CCR2. After incubation with primary antibodies, cells were centrifuged at 4°C at 1800×*g* for 4 min and washed with 200 μl of FACS buffer. After washing, cells were suspended in 200 μl of PBS, and three-color data acquisition was performed on a FACS Calibur flow cytometer. Data analyses were performed by using CellQuest software (BD).

2.4. Real-time quantitative reverse transcription–polymerase chain reaction (qRT-PCR)

Total RNA was isolated from SVCs and the liver using the RNA isolation Minikit (Qiagen) according to the manufacturer's instructions. RNA from adipocyte fraction and WAT was isolated using the Lipid Minikit (Qiagen). Total RNA (1 μg) was used to generate complementary DNA (cDNA) template using the iScript cDNA Synthesis Kit (Bio-Rad, Hercules, CA). The total reaction volume was 20 μl, with the reaction incubated in an MJ MiniCycler as follows: 5 min at 25°C, 30 min at 52°C, 5 min at 85°C and hold at 4°C. PCR was performed on cDNA using Taq DNA polymerase (Invitrogen, Carlsbad, CA) and using previously described conditions [23]. Each gene amplicon was purified with the MiniElute PCR Purification Kit (Qiagen) and quantitated on an agarose gel using a DNA mass ladder (Promega, Madison, WI). These purified amplicons were used to optimize real-time PCR conditions and to generate standard curves in real-time PCR assay. Primer concentrations and annealing temperatures were optimized for the iCycler iQ System (Bio-Rad) for each set of primers using the system's gradient protocol. PCR efficiencies were maintained between 92% and 105%, and correlation coefficients were maintained above 0.98 for each primer set (Table 1) during optimization and also during the real-time PCR of sample DNA.

cDNA concentrations for genes of interest were examined by real-time quantitative PCR using an iCycler iQ System and the iQ SYBR Green Supermix (Bio-Rad). A standard curve was generated for each gene using 10-fold dilutions of purified amplicons starting at 5 pg of cDNA and used later to

Table 1
Oligonucleotide sequences for real-time quantitative PCR

Primer	Sequence	Length	Accession number
β-ActinF	5′-CCCAGGCATTGCTGACAGG-3′	141	X03672
β-ActinR	5′-TGGAAGGTGGACAGTGAGGC-3′		
MCP-1F	5′-CTTGCCTAATCCACAGACTG-3′	146	AJ238892
MCP-1R	5′-GCCTGAACAGCACCACTA-3′		
PPARγF	5′-CAGGCTTGCTGAACGTGAAG-3′	117	NM_011146
PPARγR	5′-GGAGCACCTTGGCGAACA-3′		
CD36F	5′-CCGGGCCACGTAGAAAACA-3′	156	NM_007643
CD36R	5′-CCTCCAAACACAGCCAGGAC-3′		
TLR-4F	5′-GGCGCTCCGAGTTGTGA-3′	73	NM_009841
TLR-4R	5′-GTACCTGCTTCAGCCCAGTG-3′		

F, forward; R, reverse. PCR primer pairs were designed for 73 and 157 bp. Annealing temperatures were as follows: 57°C for β-actin, TNF-α, PPARγ, and CD36; 54°C for MCP-1 and TLR-4.
When plotting threshold cycle versus log starting quantity (pg), standard curves had slopes between −3.1 and −3.7, PCR efficiencies were between 92 and 105, and R^2 was >.98.

calculate the starting amount of target cDNA in unknown samples. SYBR Green I is a general double-stranded DNA-intercalating dye and may, therefore, detect nonspecific products and primers/dimers in addition to the amplicon of interest. In order to determine the number of products synthesized during real-time PCR, a melting curve analysis was performed on each product. Real-time PCR was used to measure the starting amount of nucleic acid of each unknown sample of cDNA on the same 96-well plate. Results are presented as the starting quantity of target cDNA (picograms) per microgram of total RNA.

2.5. Hepatic steatosis, plasma MCP-1 and liver TG content

Liver specimens were excised and immediately fixed in 10% phosphate-buffered neutral formalin, embedded in paraffin, cut at thicknesses of 5 μm and stained with hematoxylin and eosin (H&E) for histological examination. For hepatic TG assessment, livers fragments (50–100 mg) were extracted for 16 h at 4°C with 4 ml of $CHCl_3$/methanol (2:1, vol/vol). Two milliliters of 0.6% NaCl was then added to the extract, and the mixture was centrifuged at 2000×*g* for 20 min. Lipids were isolated by nitrogen evaporation, dissolved in 100 μl of isopropanol and quantified with the Triglyceride Assay Kit (Stanbio). The Triglyceride Assay Kit (Sigma) and Ready–Set–Go MCP-1 ELISA (eBioscience) were used to quantify plasma TGs and MCP-1, respectively, according to the manufacturer's instructions.

2.6. Transfection of 3T3-L1 preadipocytes

A pCMX.PPARγ expression plasmid (kindly provided by Dr. R.M. Evans; The Salk Institute, San Diego, CA) and pMCP-1-514(enh) luc construct [24] were purified using Qiagen's Maxi kit. 3T3-L1 cells (American Type Culture Collection, Manassas, VA) were grown in 24-well plates in DMEM high-glucose medium (Invitrogen) containing 10% fetal bovine serum (FBS) until 60–70% confluence. Before transfection, the medium was changed to 1% FBS. The cells cultured in 24-well plates were cotransfected with 0.8 μg of plasmid DNA and 1 ng of pRL reporter control plasmid per well using F-1 transfection reagents (Targeting Systems, Santee, CA) according to the manufacturer's protocol. Transfection efficiencies were determined by cotransfecting cells with a pcDNA 3.1/His/*lac*Z control vector at 24 h. Transfected cells were then treated with either a racemic ABA mixture (12.5 μM; Sigma) or rosiglitazone (1 μM; Cayman Chemicals, Ann Arbor, MI) for 24 h. Designated wells were also treated with the PPARγ antagonist GW9662 (30 μM; Cayman Chemicals). Transfected cells were

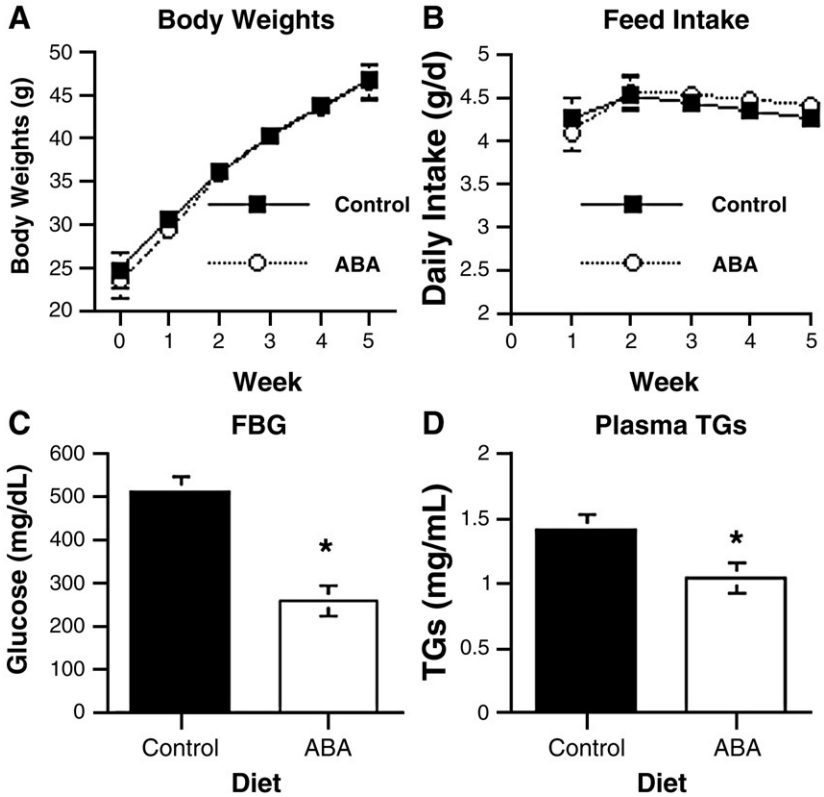

Fig. 1. ABA ameliorates fasting glucose concentrations without inducing body weight gain. Effect of ABA on body weight, feed intake, FBG and plasma lipids. Db/db mice were fed control or ABA-supplemented (100-mg/kg diet) high-fat diets for 36 days. (A) Body weights and (B) food intake were assessed weekly. After dietary treatment, plasma was withdrawn from fasted mice (12 h) to obtain (C) FBG (mg/dl) and (D) plasma TGs (mg/ml). Data are presented as least squares mean±S.E. of 10 mice. The error bars at some time points (A and B) are smaller than the symbols and cannot be seen in the figure. Data points with an asterisk are significantly different ($P<.05$).

harvested in reporter lysis reagent. Luciferase activity, normalized to pRL activity in cell extracts, was determined by using the dual luciferase reporter assay system (Promega) in a TD-20/20 Single-Tube Luminometer (Turner Biosystems, Sunnyvale, CA). Relative luciferase activity was calculated as the ratio of chemiluminescence 10 s after the Luciferase Assay Reagent II (Promega) to chemiluminescence 10 s after the Stop&Glo Reagent (Promega).

2.7. Statistical analyses

For db/db experiment, data were analyzed as a completely randomized design. To determine the statistical significance of the model, analysis of variance (ANOVA) was performed using the general linear model procedure of Statistical Analysis Software (SAS). In the experiment using PPARγ fl/fl, MMTV-Cre^{+}/PPARγ fl/fl and MMTV-Cre^{-} mice, data were analyzed as a 2×2 factorial arrangement within a completely randomized design. The statistical model utilized was: $Y_{ijk}=\mu+\text{genetic background}_i+\text{diet}_j+(\text{genetic background}\times\text{diet})_{ij}+\text{error}_{ijk}$. To determine the statistical significance of the model, ANOVA was performed using the general linear model procedure of SAS, and the probability value (P) of <.05 was considered significant. When the model was significant, ANOVA was followed by Fisher's Protected Least Significant Difference multiple comparison method. Nonparametric data were analyzed by the Mann–Whitney U test followed by Dunn's multiple comparisons test.

3. Results

3.1. ABA improves fasting glucose and lowers plasma TGs in db/db mice without affecting body weight

ABA supplementation to db/db mice for 36 days significantly lowers fasting glucose levels and improves their response to intraperitoneal GTT [21]. Similar to these previous findings, ABA did not alter the food intake or body weights of db/db mice throughout the course of the experiment (Fig. 1A and B). In this study, db/db mice fed the ABA-supplemented diet had significantly lower FBG and plasma TG concentrations when compared to mice fed the control high-fat diet (Fig. 1C and D).

3.2. The stromal–vascular fraction (SVF) contains two phenotypically distinct macrophage subpopulations

To characterize phenotypical differences in ATM in the SVF, we examined the surface expression of F4/80, CD11b and CCRs (CCR2 and CCR5). SVCs were isolated from adipocytes by gradient centrifugation and subsequently gated on the immune cell population based on forward-versus-side scatter (Fig. 2A). We identified two phenotypically distinct

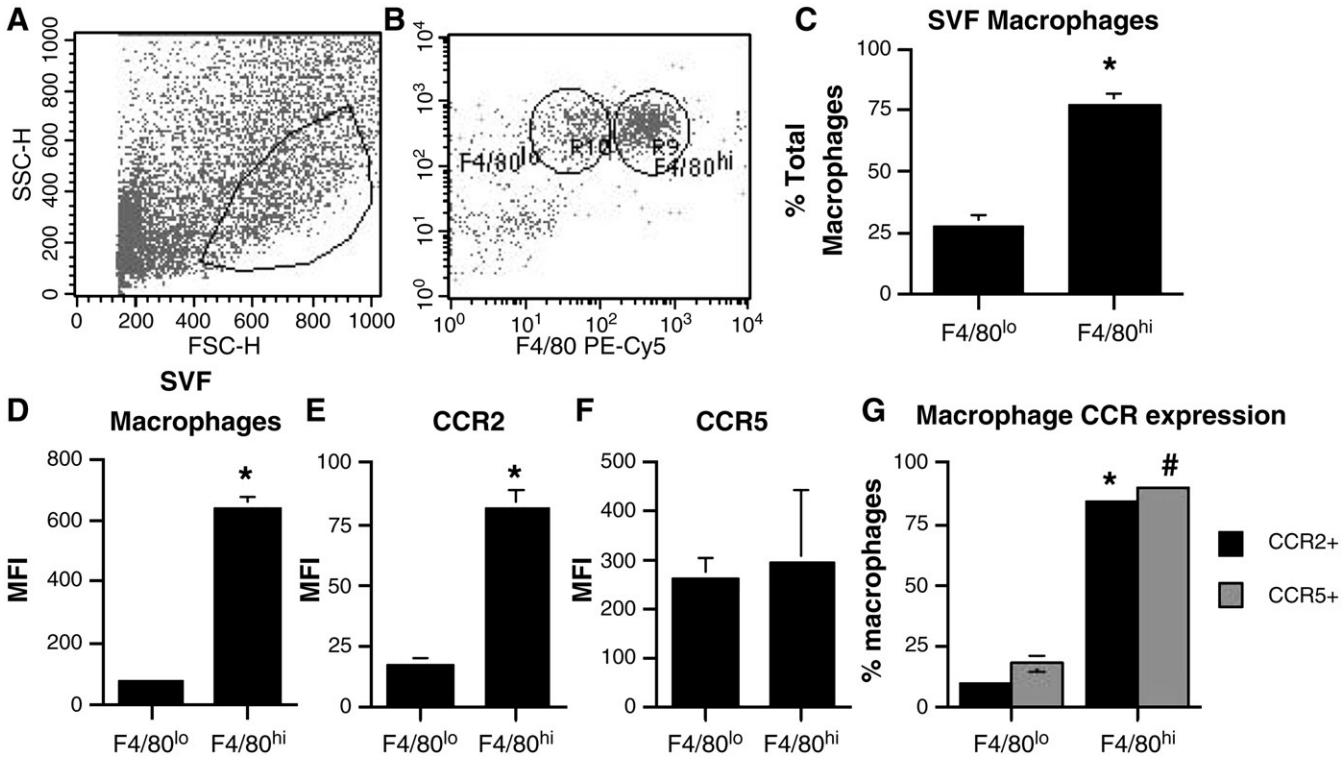

Fig. 2. Phenotypic analysis of macrophage subsets within the SVF of WAT. (A and B) Representative dot plots from a control db/db mouse. The F4/80^{hi} and F4/80^{lo} subsets differed significantly in (C) the total amount of macrophages and (D) MFIs. (E and F) MFIs of CCR2-expressing and CCR5-expressing macrophages in each population, respectively. (G) The percentage of macrophages in each population expressing either CCR2 or CCR5. Data are presented as least squares mean±S.E. of 10 observations. Data points with an asterisk or number sign indicate a significant difference (P<05) between separate macrophage populations.

subpopulations of F4/80^{+} CD11b^{+} macrophages in the SVF of WAT that differed in their mean fluorescence intensity (MFI) for F4/80, yielding a macrophage subset expressing high surface concentrations of the F4/80 molecule (F4/80^{hi}) and a subset expressing low surface concentrations of the F4/80 molecule (F4/80^{lo}) (Fig. 2B and C). The F4/80^{hi} population was more abundant in WAT than in the F4/80^{lo} subset, encompassing approximately 75% of total macrophages versus 25% in control-fed db/db mice, respectively (Fig. 2B). The F4/80^{hi} macrophage subset also expressed higher surface concentrations of CCR2 and CCR5 when compared to the F4/80^{lo} subset (Fig. 2G).

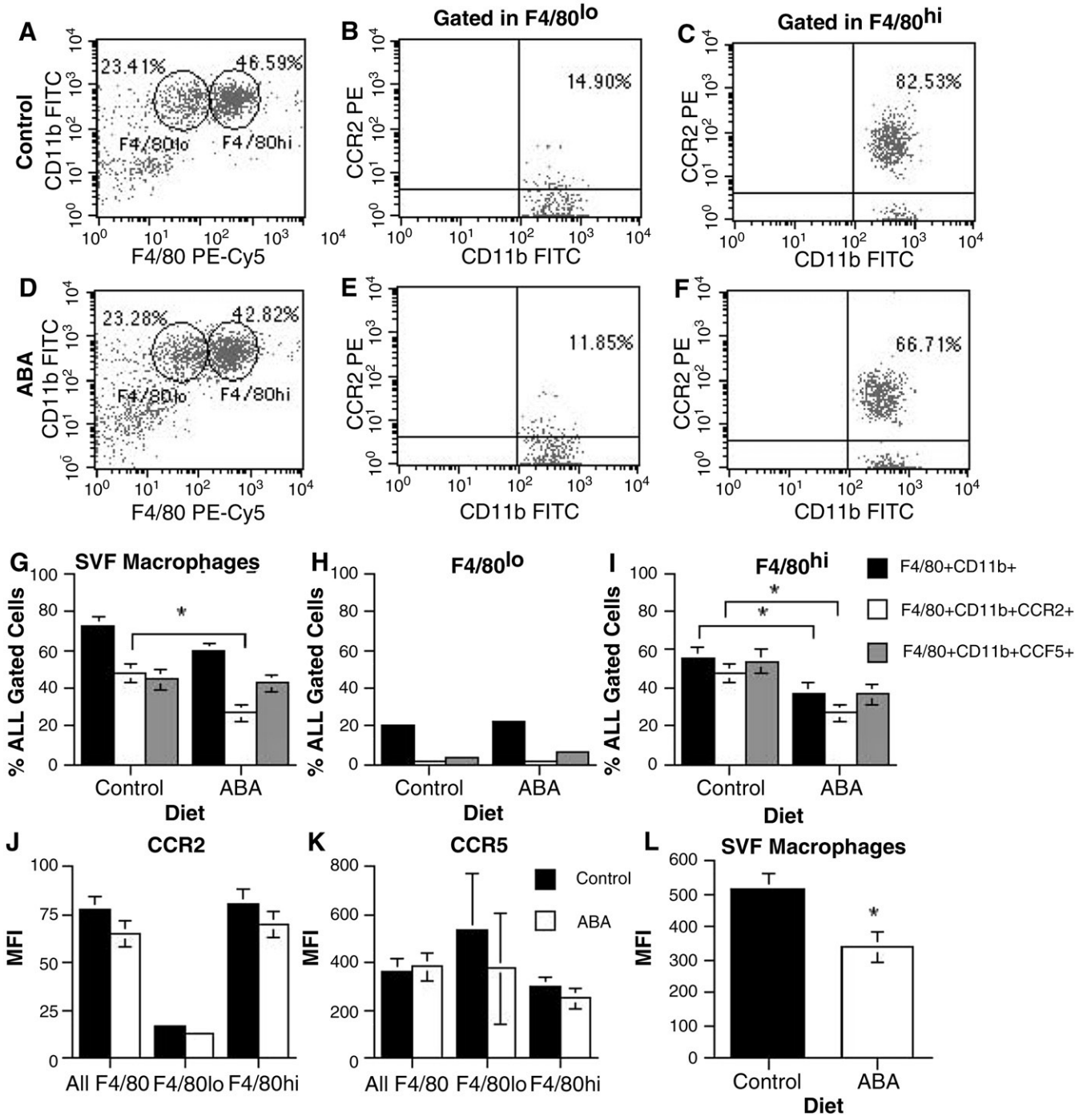

Fig. 3. ABA decreases the numbers of F4/80^{hi} macrophages in WAT. (A–C) Representative dot plots for total SVF macrophage infiltration and the percentages of CCR2^{+} macrophages in the F4/80^{hi} and F4/80^{lo} subsets, respectively, for control-fed db/db mice. (D–F) The respective dot plots for a representative ABA-fed db/db mouse. (G–I) The contribution of SVF macrophages, F4/80^{lo} macrophages and F4/80^{hi} macrophages to the total amount of gated cells. The MFIs of each macrophage subpopulation for (J) CCR2 and (K) CCR5. (L) The difference in the MFI of total SVF macrophages between control and ABA-fed mice. Data are presented as least squares mean±S.E. of 10 observations. Data points with different superscripts are significantly different (P<.05).

3.3. ABA inhibits F4/80^{hi} macrophage infiltration into WAT

After characterizing these two macrophage subpopulations, we next determined whether ABA targeted one of these populations or both. We found that ABA significantly suppressed F4/80^{hi} macrophage infiltration into WAT (P=.05) but had no effect on F4/80^{lo} ATM (Fig. 3). In addition, the amount of F4/80 expressed in the surface of F4/80^{hi} macrophages administered ABA, as measured by MFI, was significantly lower than that in mice fed the control diet (Fig. 3L). The differences observed in the F4/80^{hi} population in mice fed ABA were due primarily to a reduction in a subset of F4/80^{hi} CD11b^{+} CCR2^{+} ATM (P=.006).

3.4. ABA decreases MCP-1 mRNA expression in WAT and MCP-1 protein concentrations in plasma, and attenuates liver TG accumulation and hepatic steatosis

A significant reduction in the infiltration of the F4/80^{hi} CD11b^{+} CCR2^{+} macrophage subset into WAT could be due to attenuated CCR2 surface expression in monocytes, repression of CCR2 ligand expression in WAT, or both.

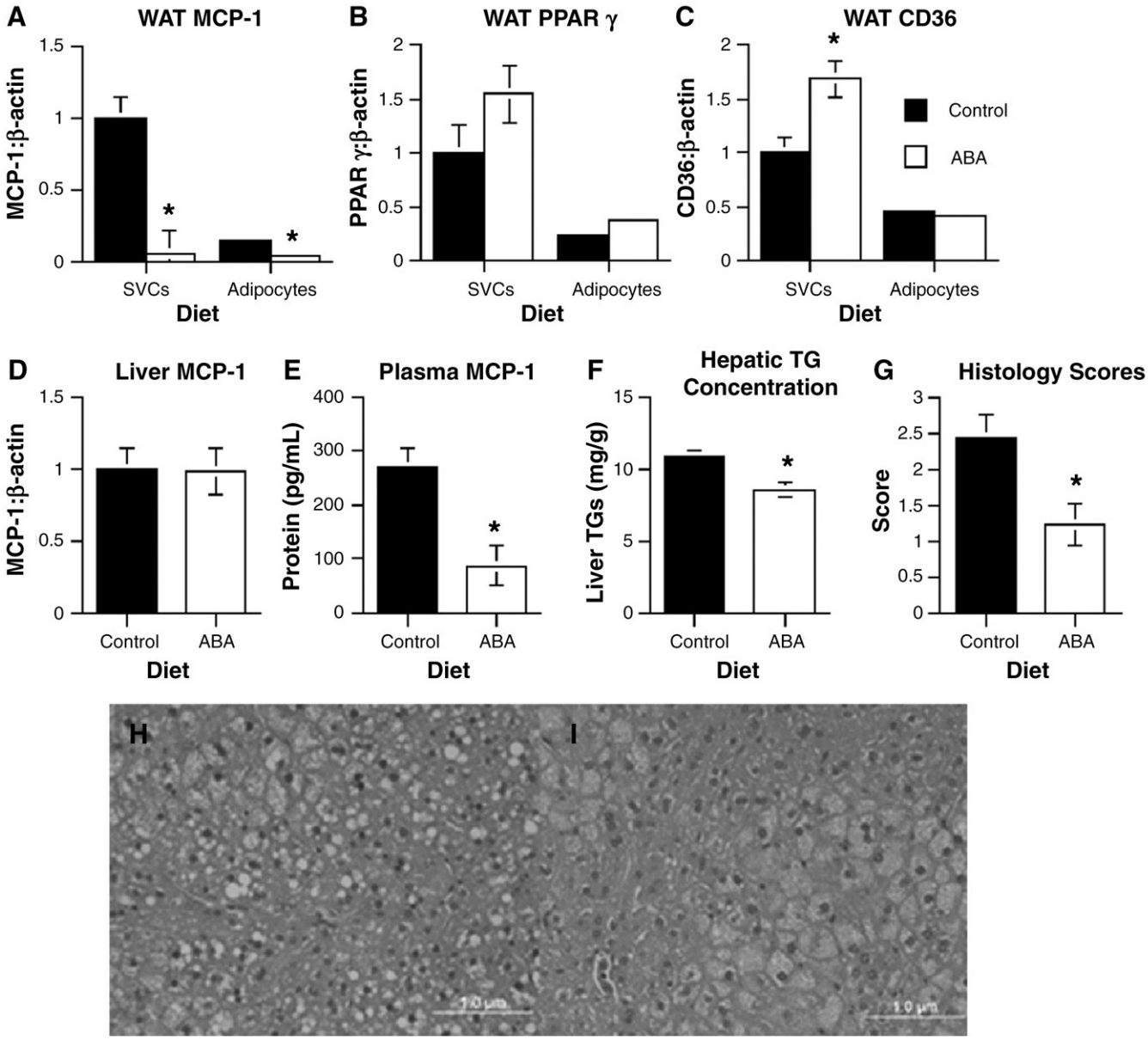

Fig. 4. ABA induces PPARγ and suppresses the expression of MCP-1 in WAT. Effect of dietary ABA supplementation on WAT and liver gene expression, MCP-1 protein levels, liver TG concentrations and hepatic steatosis scores. Db/db mice were fed high-fat diets with (black bars) or without (empty bars) ABA (100 mg/kg) for 36 days. Gene expression in RNA isolated from SVCs and adipocytes was analyzed by real-time qRT-PCR for (A) MCP-1, (B) PPARγ and (C) CD36. (D) Liver MCP-1 expression, (E) plasma MCP-1 (pg/ml) and (F) liver TGs (mg/g tissue) were also assessed. Gene expression values are expressed as a relative ratio to the housekeeping gene *β-actin*. Data are presented as least squares mean±S.E. of 10 observations. Data points with an asterisk are significantly different (P<.05). (G) Liver histology scores. (H and I) Representative photomicrographs of liver histology specimens stained with H&E.

CCR2 and its principal ligand MCP-1 have been recently linked to the development of obesity-induced insulin resistance [17–19]. To determine whether ABA inhibited MCP-1 expression in WAT, we assessed levels of MCP-1 mRNA content in the SVF (i.e., macrophages, T cells, fibroblasts, preadipocytes and endothelial cells) and in the adipocyte fraction. Both WAT fractions produce MCP-1 in obese mice and humans [2]. We found that ABA decreased the concentrations of MCP-1 mRNA by almost 15-fold in SVCs. There was also a significant reduction in MCP-1 mRNA in the adipocyte fraction following ABA supplementation (P=.05), although this reduction was not as drastic as the difference observed in SVCs (Fig. 4A). PPARγ mRNA expression was higher in both SVCs and adipocytes (Fig. 4B), but expression of the well-known PPARγ-responsive gene and fatty acid transporter CD36 was only significantly elevated in SVCs (Fig. 4C). We did not see significant differences in the mRNA expression of MIP-1α or the innate immune receptor toll-like receptor 4 (TLR-4) in either SVCs or adipocytes (data not shown).

We next determined whether the suppressed MCP-1 expression observed in WAT of ABA-fed mice resulted in decreased plasma MCP-1 concentrations. MCP-1 protein concentrations were significantly decreased in plasma, but not in the liver, from ABA-fed mice (Fig. 4D and E),

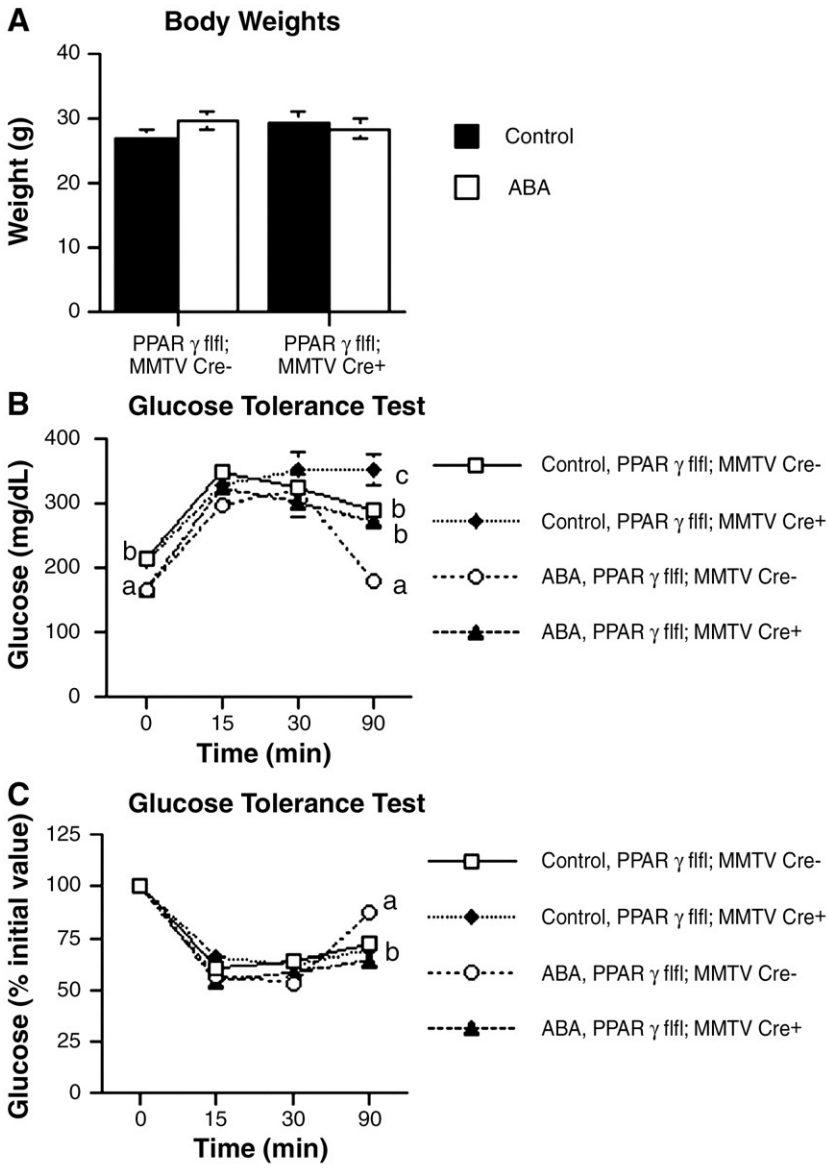

Fig. 5. The beneficial effects of ABA on insulin resistance are abrogated in immune-cell-specific PPARγ-null mice. PPARγ fl/fl, MMTV-Cre^{+}/PPARγ fl/fl and MMTV-Cre^{-} littermates (wild-type phenotype) were fed high-fat diets with or without ABA (100 mg/kg). (A) Final body weights and (B) response to intraperitoneal glucose challenge (2 g glucose/kg body weight) in fasted mice (6 h) were assessed after 28 weeks of dietary supplementation. Data are presented as least squares mean±S.E. of eight mice. The error bars at some time points (B and C) are smaller than the symbols and cannot be seen in the figure. Data points with different superscripts are significantly different (P<.05).

suggesting that WAT-derived MCP-1 may elicit systemic actions. In a recent study, MCP-1-overexpressing mice under the control of the aP2 promoter (i.e., adipose tissue specific) had a significantly elevated risk of developing hepatic steatosis [18]. Upon histological examination of liver specimens, we found that hepatic steatosis was less severe in ABA-fed mice (Fig. 4G). In line with this histological finding, the amount of liver TGs was significantly lower in mice fed the ABA-supplemented diet than in mice fed the control diet (Fig. 4F).

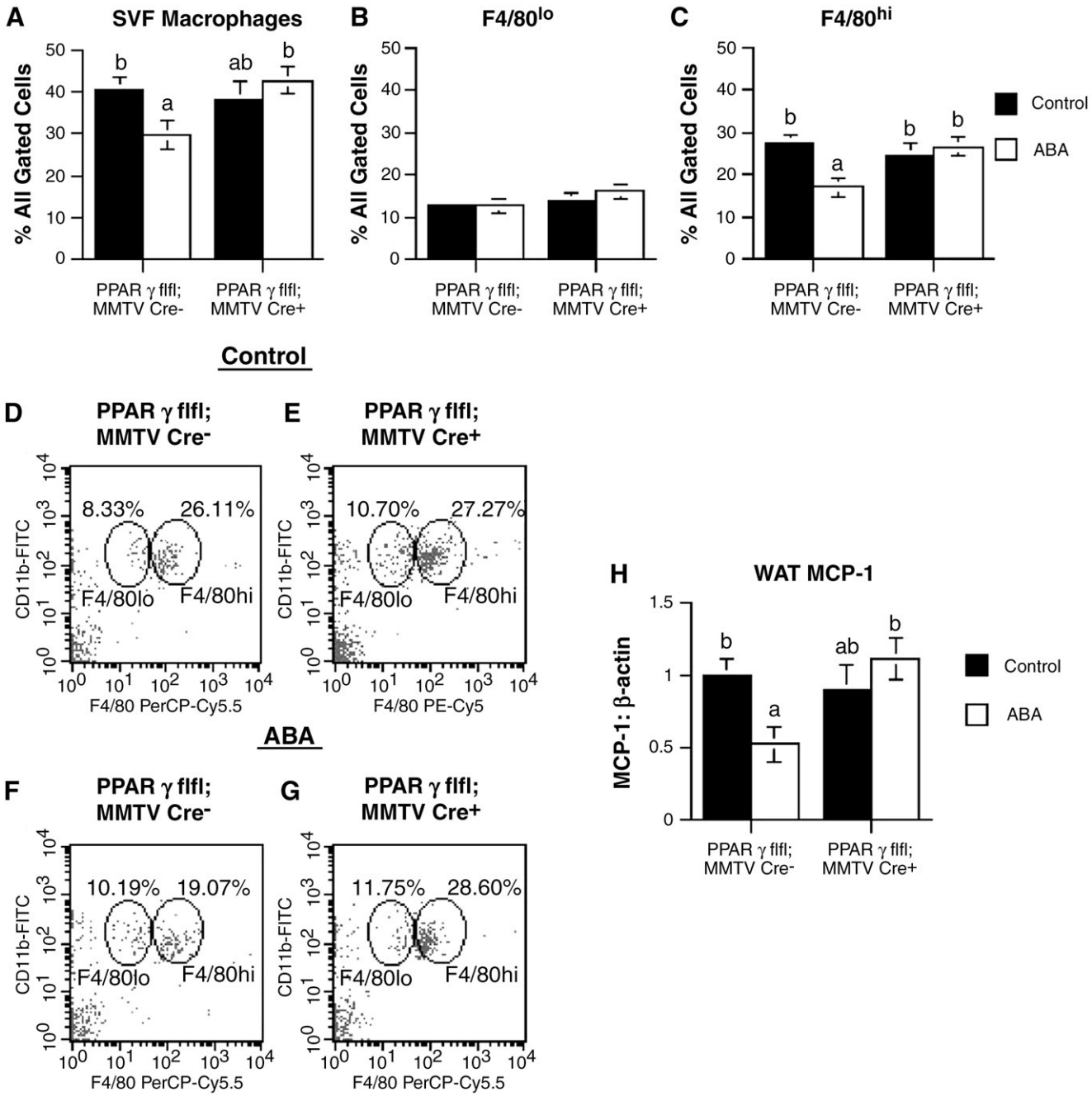

Fig. 6. The beneficial effects of ABA on the infiltration of monocytes and chemokine production in WAT are abrogated in immune-cell-specific PPARγ-null mice. Effect of dietary ABA supplementation and tissue-specific deletion of PPARγ in immune cells on ATM phenotype. (A–C) The effects of ABA on total macrophage infiltration and the percentage of F4/80^{lo} and F4/80^{hi} ATMs in PPARγ fl/fl, MMTV-Cre^{+}/PPARγ fl/fl and MMTV-Cre^{-} mice. (D and E) Representative dot plots for SVF infiltration of ATMs in PPARγ fl/fl, MMTV-Cre^{+}/PPARγ fl/fl and MMTV-Cre^{-} mice fed the control high-fat diet. (F and G) The respective dot plots for ABA-fed mice. Real-time qRT-PCR was used to assess the expression of MCP-1 (H). Data are presented as least squares mean±S.E. of eight mice. The error bars at some time points (B) are smaller than the symbols and cannot be seen in the figure. Data points with different superscripts are significantly different (P<.05).

3.5. Targeted deficiency of PPARγ expression in immune cells impairs the ability of ABA to improve glucose tolerance

The greatest differences in MCP-1 and the PPARγ-responsive gene *CD36* induced by ABA occurred in SVCs, suggesting that immune cell PPARγ (and not adipocyte PPARγ) is the molecular target for ABA in WAT. To determine whether the ability of ABA to normalize plasma glucose concentrations following GTT was mediated through immune cell PPARγ, we next fed high-fat diets supplemented with or without ABA to PPARγ fl/fl and MMTV-Cre^{+} mice, which do not express PPARγ in hematopoietic cells, and in PPARγ fl/fl and MMTV-Cre^{-} littermates (wild-type phenotype). After 28 weeks of high-fat feeding, the mice were overweight (Fig. 5A). Similar to our findings with db/db mice, ABA did not increase body weights in either MMTV-Cre^{+} and MMTV-Cre^{-} and did not effect food intake (data not shown). The deficiency of PPARγ in immune cells abrogated ABA-induced normalization of FBG concentrations 90 min following intraperitoneal GTT (Fig. 5B and C).

3.6. Deficient PPARγ expression in immune cells impairs the ability of ABA to suppress MCP-1 expression and infiltration of the F4/80^{hi} macrophage subset into WAT

To determine whether the observed differences in glucose tolerance corresponded to phenotypic changes in SVF macrophage subsets, we investigated the effect of ABA on both F4/80^{hi} and F4/80^{lo} ATM. Dietary ABA supplementation significantly decreased both total SVF macrophage infiltration and the amount of F4/80^{hi} macrophages in mice expressing PPARγ in immune cells (i.e., PPARγ fl/fl and MMTV-Cre^{-}). However, the deficiency of PPARγ in immune cells (i.e., PPARγ fl/fl and MMTV-Cre^{+}) abrogated the ability of ABA to suppress the infiltration of F4/80^{hi} into WAT. Of note, surface CCR2 was expressed by a greater percentage of ATMs from tissue-specific PPARγ-null mice (data not shown).

We next examined whether immune cell PPARγ was required for the suppressive actions of ABA on WAT MCP-1 mRNA expression. ABA decreased both WAT and plasma MCP-1 levels in mice expressing PPARγ in immune cells (Fig. 6H). However, in line with our findings on F4/80^{hi} macrophage infiltration into WAT, the ability of ABA to suppress the expression of MCP-1 in WAT was significantly impaired in tissue-specific PPARγ-null mice, suggesting that ABA acts through a mechanism requiring the expression of PPARγ in immune cells. The SVF of WAT contains macrophages, T cells, endothelial cells, fibroblasts and preadipocytes, but the only cell subsets in this fraction lacking the *PPARγ* gene in the tissue-specific PPARγ-null mouse would be cells of hematopoietic origin (i.e., bone-marrow-derived macrophages and T cells). Thus, the observed differences in glucose tolerance might be attributed to one or both immune cell subsets.

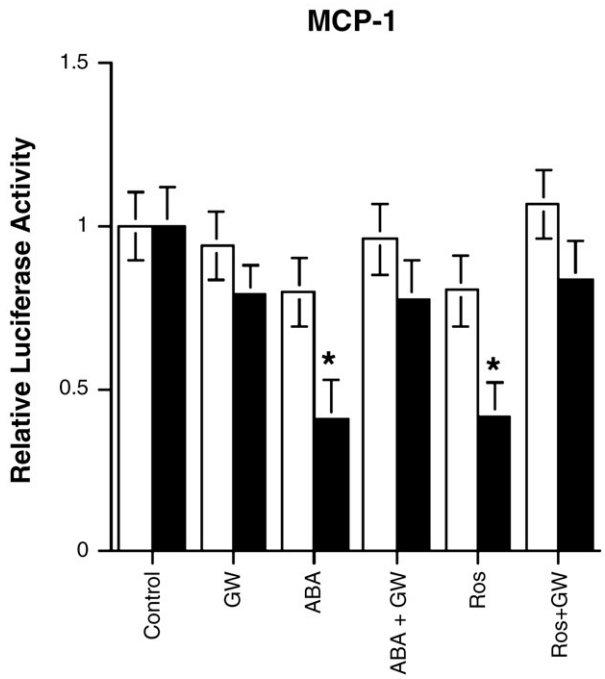

Fig. 7. ABA inhibits MCP-1 promoter activity by acting through PPARγ. 3T3-L1 preadipocytes were transfected with an MCP-1 promoter luciferase reporter construct with (black bars) or without (empty bars) cotransfection with a pCMX.PPARγ expression plasmid. After 20 h, cells were treated with the PPARγ antagonist GW9662 (GW; 30 μM), ABA (12.5 μM), rosiglitazone (Ros; 1 μM), ABA and GW, or Ros and GW. The results were normalized for *Renilla* activity. Data are presented as least squares mean±S.E. of four observations. Data points with an asterisk are significantly different ($P<.05$).

3.7. ABA inhibits MCP-1 promoter activity through PPARγ

To further examine the effect of ABA on MCP-1 transactivation, 3T3-L1 preadipocytes were transfected with an MCP-1 promoter luciferase reporter construct and cotransfected with a pCMX.PPARγ expression plasmid to increase endogenous PPARγ activity. Cells were then treated with ABA (12.5 μM), rosiglitazone (1 μM), the PPARγ antagonist GW9662 (30 μM) or a combination of agonist and inhibitor. We previously found that ABA (12.5 μM) and rosiglitazone (1 μM) were equally effective in inducing PPARγ transactivation [21]. In this study, cotransfection with the PPARγ expression vector significantly enhanced the ability of both ABA and rosiglitazone to inhibit MCP-1 promoter activity (Fig. 7). The effects of both compounds on MCP-1 transactivation were significantly inhibited by cotreatment with GW9662.

4. Discussion

The obesity and T2D epidemics follow a similar demographic pattern [1,25], but little is known about the factors linking obesity to insulin resistance and T2D at the cellular and molecular levels. The “FFA efflux theory” proposes that adipocyte dysfunction and extra adipose fat

storage are the central components in the pathogenesis of insulin resistance, highlighting the importance of adipocytes as cellular targets [26–28]. In contrast, the "endocrine theory" suggests that pro-inflammatory mediators play an essential immunopathogenic role, favoring immune cells as central cellular targets for therapies against T2D [29]. PPARγ is expressed in both adipocytes and immune cells, and has been identified as an important therapeutic target in both insulin resistance and T2D. In this report, we show that PPARγ and its responsive gene *CD36* are expressed at higher concentrations in SVCs than in adipocytes, and that treatment with a novel insulin-sensitizing PPARγ agonist induces PPARγ-responsive gene expression primarily in SVCs. These results are also suggestive that TZDs may elicit their insulin-sensitizing actions through PPARγ expressed in immune cells infiltrating the WAT. Hence, PPARγ activation in immune cells may be a central regulator of insulin resistance and obesity-related inflammation. In line with this hypothesis, obesity-induced insulin resistance is associated with the infiltration of bone-marrow-derived monocytes into WAT and with differentiation into ATM [2,5]. This study phenotypically characterized the subsets of ATM targeted by ABA and investigated whether this compound ameliorates insulin resistance and obesity-related inflammation through a mechanism dependent upon immune cell PPARγ.

We have previously found that ABA improves glucose tolerance and reduces total ATM infiltration and TNF-α expression in WAT of db/db mice [21]. To phenotypically characterize the actions of ABA on the ATM population, we presently isolated SVCs from WAT and assayed their expression of the glycoproteins F4/80 and CD11b and of CCR2 and CCR5. F4/80 contains extracellular epidermal-growth-factor-like domains and a seven-span transmembrane (TM7) domain; it has been suggested to play a role in cell adhesion and cell signaling, and it is widely used as a maturation marker for macrophages [30]. We report for the first time the presence of two phenotypically distinct subsets of macrophages in the SVF of WATs, which differ in the amount of surface F4/80 (e.g., F4/80^{lo} and F4/80^{hi}). The newly identified F4/80^{hi} subset is more abundant (i.e., 75% of macrophages in the SVF) and expresses higher surface concentrations of CCR2 and CCR5 in comparison to the F4/80^{lo} population.

The expression of F4/80 is tightly regulated according to the physiological status of cells. Because the precursor of tissue macrophages (the bone-marrow-derived blood monocyte) expresses lower surface F4/80 than its mature counterparts [30], the F4/80^{hi} ATM subset is probably a mature cell type that contributes to obesity-related inflammation, whereas F4/80^{lo} ATM may comprise monocytes that have recently transmigrated into the WAT. Alternatively, a difference in the ontogeny of F4/80^{hi} and F4/80^{lo} macrophages could account for these two distinct ATM subsets. The SVF, in addition to containing bone-marrow-derived cells of myeloid origin, includes preadipocytes that can differentiate into adipocytes or F4/80-expressing macrophages of mesenchymal origin [31]. Resident macrophages from different organs differ considerably in the amount of F4/80 expressed on their surfaces [32]. Moreover, the limited expression of CCRs on the majority of F4/80^{lo} ATMs may be indicative of a predominantly resident population [33].

After phenotypically characterizing these two ATM subsets, we next examined the ability of ABA to differentially modulate their numbers in WAT. We found that ABA decreased the amount of F4/80^{hi} CCR2^{+} ATM but had a negligible effect on the F4/80^{lo} population. Although the effect of synthetic PPARγ ligands on the infiltration of F4/80^{hi} CCR2^{+} ATM has not been studied, the reduction of this subset of ATM by ABA is in line with the well-characterized ability of PPARγ to suppress CCR2 expression. At the molecular level, the *CCR2* gene contains two promoters that are both repressed by PPARγ [16], and TZDs down-regulate MCP-1-induced chemotactic response in THP-1 monocytes [34]. Moreover, in obese mice matched for adiposity, *Ccr2* deficiency decreased macrophage content and WAT inflammation while ameliorating hepatic steatosis [17]. We propose that ABA activates PPARγ in monocytes, which in turn suppresses surface CCR2 expression and infiltration of F4/80^{hi} ATM.

We next determined whether ABA down-regulated the expression of MCP-1, the main ligand for CCR2, in WAT. Similar to CCR2, MCP-1 is inhibited following TZD treatment in both SVCs and adipocytes [35]. We found a 15-fold decrease in MCP-1 mRNA in the SVF of WAT and a 4-fold decrease in plasma MCP-1. The decrease observed in SVCs was far greater than the approximately twofold decrease Xu et al. [5] obtained following similar short-term intervention with rosiglitazone in ob/ob mice. In addition to recruiting macrophages and directly impairing insulin signaling by blocking IRS-1 and Akt phosphorylation [19], MCP-1 has been recently shown to increase the risk for hepatic steatosis by activating the gluconeogenic genes phosphoenolpyruvate carboxykinase (*PEPCK*) and glucose-6-phosphatase (*G6P*) and by preserving lipid storage capacity [18]. In line with the suppressed expression of MCP-1 mRNA in WAT and the decreased concentrations of MCP-1 protein in the plasma of ABA-fed mice, we observed a decreased severity in high-fat-diet-induced hepatic steatosis that could not be attributed to differences in MCP-1 mRNA expression in the liver. In addition to decreased systemic MCP-1 concentrations, ABA-induced reduction in plasma TGs may contribute to the improvement of liver steatosis. To further characterize the role of PPARγ in mediating ABA-induced repression of MCP-1, we cotransfected 3T3-L1 preadipocytes with an MCP-1 reporter construct and a PPARγ expression vector. The presence of the expression vector significantly enhanced the ability of both ABA and rosiglitazone to inhibit MCP-1 promoter activity. The effects of both compounds were also inhibited by the selective PPARγ antagonist GW9662. Because the MCP-1 promoter is not known to contain PPRE (peroxisome proliferator response element), the inhibition of MCP-1 promoter activity

may have occurred though PPARγ-induced inhibition of NF-κB-responsive genes. In 2005, Pascual et al. [36] demonstrated that, following ligand binding, the PPARγ ligand-binding domain becomes sumoylated, resulting in its migration to nuclear receptor corepressor (NCoR)–histone deacetylase-3 complexes on inflammatory gene promoters. The presence of PPARγ at these sites inhibited the ubiquitination of NCoR, which is required for NF-κB-induced transcription of pro-inflammatory genes [36].

Because macrophages are the main producers of MCP-1 in WAT, we next examined whether the deletion of PPARγ in immune cells would impair the ability of ABA to ameliorate insulin resistance and obesity-related inflammation. For this purpose, we used a mouse model in which the *PPARγ* gene has been disrupted in immune cells. While several studies have been performed on muscle-specific [37] and adipose-tissue-specific PPARγ-null mice [38], little is known about the importance of immune cell PPARγ in the regulation of insulin resistance and T2D. PPARγ fl/fl and MMTV-Cre^{+} mice lack PPARγ in immune and epithelial cells but express it at normal concentrations in adipocytes. Thus, they represent an excellent model to dissect the immune-cell-dependent mechanisms of PPARγ action. We have previously used this loss-of-function approach to characterize in vivo the mechanism by which conjugated linoleic acid, another natural agonist of PPARγ, prevents intestinal inflammation [23]. Our present findings indicate that the loss of PPARγ in immune cells impairs the ability of ABA to improve glucose tolerance, suppress F4/80^{hi} ATM infiltration and down-regulate MCP-1 expression in WAT, suggesting that the protective actions of ABA on insulin resistance are mediated, in part, through a mechanism dependent upon the expression of PPARγ in immune cells. These findings, however, do not preclude that possibility that ABA can also activate other extracellular or intracellular receptors to induce its insulin-sensitizing effects, and current work in our laboratory is being conducted to explore these options. Moreover, since we have observed that fasting glucose levels were improved by ABA supplementation in both Cre^{+} and Cre^{-} mice, other cells and tissues, including adipocytes, preadipocytes, skeletal muscle, liver and others, may have played a role in the beneficial effects of ABA.

In summary, we have characterized for the first time two phenotypically distinct subsets of ATM (F4/80^{hi} and F4/80^{lo}) and have demonstrated that a novel PPARγ agonist decreases the infiltration of F4/80^{hi} ATM, MCP-1 expression in WAT and MCP-1 promoter activity, and ameliorates insulin resistance through a mechanism requiring immune cell PPARγ. These data further support the theory that immune-cell-derived pro-inflammatory mediators are essential components in the pathogenesis of insulin resistance and T2D. While our data show that F4/80^{hi} ATMs are important contributors to the immunopathogenesis of insulin resistance, additional work is needed to characterize the role of other immune cell subsets (i.e., natural killer cells, dendritic cells and regulatory T cells) in modulating this abnormal immune response. Of particular interest are infiltrating regulatory T cells given their higher concentrations of PPARγ when compared to other T cell subsets and their ability to suppress established inflammation. Uncovering immunoregulatory mechanisms, such as PPARγ action, by which insulin resistance can be prevented may take us one step closer to halting the epidemics of insulin resistance and T2D.

Acknowledgments

This study was supported by a grant from the Institute for Biomedical and Public Health Sciences (awarded to J.B.-R.) and funds from the Nutritional Immunology and Molecular Nutrition Laboratory. Support was also provided by the John Lee Pratt Fellowship program.

The authors would like to thank Dr. Kathryn Reynolds for her technical assistance in this project; Drs. Frank Gonzalez, Yongzhi Cui and Lothar Hennighausen for kindly providing the initial PPARγ floxed and MMTV-Cre breeder pairs; and Dr. R.M. Evans for kindly providing the PPARγ expression vector. We would also like to thank Drs. Liwu Li and Kevin Davy for critical reading of the manuscript and for constructive comments.

References

[1] Center for Disease Control and Prevention. National Diabetes Fact Sheet: general information and national estimates on diabetes in the United States, 2005. Atlanta, GA: US Department of Health and Human Services, Center for Disease Control and Prevention; 2005. p. 1–10.
[2] Weisberg SP, McCann D, Desai M, Rosenbaum M, Leibel RL, Ferrante Jr AW. Obesity is associated with macrophage accumulation in adipose tissue. J Clin Invest 2003;112:1796–808.
[3] Cinti S, Mitchell G, Barbatelli G, Murano I, Ceresi E, Faloia E, et al. Adipocyte death defines macrophage localization and function in adipose tissue of obese mice and humans. J Lipid Res 2005;46: 2347–55.
[4] Bruun JM, Lihn AS, Pedersen SB, Richelsen B. Monocyte chemoattractant protein-1 release is higher in visceral than subcutaneous human adipose tissue (AT): implication of macrophages resident in the AT. J Clin Endocrinol Metab 2005;90:2282–9.
[5] Xu H, Barnes GT, Yang Q, Tan G, Yang D, Chou CJ, et al. Chronic inflammation in fat plays a crucial role in the development of obesity-related insulin resistance. J Clin Invest 2003;112:1821–30.
[6] Gerhardt CC, Romero IA, Cancello R, Camoin L, Strosberg AD. Chemokines control fat accumulation and leptin secretion by cultured human adipocytes. Mol Cell Endocrinol 2001;175:81–92.
[7] Lehmann JM, Moore LB, Smith-Oliver TA, Wilkison WO, Willson TM, Kliewer SA. An antidiabetic thiazolidinedione is a high affinity ligand for peroxisome proliferator-activated receptor gamma (PPAR gamma). J Biol Chem 1995;270:12953–6.
[8] Desvergne B, Wahli W. Peroxisome proliferator-activated receptors: nuclear control of metabolism. Endocr Rev 1999;20:649–88.
[9] Yamauchi T, Kamon J, Waki H, Murakami K, Motojima K, Komeda K, et al. The mechanisms by which both heterozygous peroxisome proliferator-activated receptor gamma (PPARgamma) deficiency and PPARgamma agonist improve insulin resistance. J Biol Chem 2001; 276:41245–54.
[10] Otto TC, Lane MD. Adipose development: from stem cell to adipocyte. Crit Rev Biochem Mol Biol 2005;40:229–42.
[11] Lehrke M, Lazar MA. The many faces of PPARgamma. Cell 2005;123: 993–9.

[12] Guri AJ, Hontecillas R, Bassaganya-Riera J. Peroxisome proliferator-activated receptors: bridging metabolic syndrome with molecular nutrition. Clin Nutr 2006; doi:10.1016/j.clnu.2006.08.006.
[13] Braissant O, Foufelle F, Scotto C, Dauca M, Wahli W. Differential expression of peroxisome proliferator-activated receptors (PPARs): tissue distribution of PPAR-alpha, -beta, and -gamma in the adult rat. Endocrinology 1996;137:354–66.
[14] Welch JS, Ricote M, Akiyama TE, Gonzalez FJ, Glass CK. PPARgamma and PPARdelta negatively regulate specific subsets of lipopolysaccharide and IFN-gamma target genes in macrophages. Proc Natl Acad Sci U S A 2003;100:6712–7.
[15] Knowler WC, Hamman RF, Edelstein SL, Barrett-Connor E, Ehrmann DA, Walker EA, et al. Prevention of type 2 diabetes with troglitazone in the Diabetes Prevention Program. Diabetes 2005;54:1150–6.
[16] Chen Y, Green SR, Ho J, Li A, Almazan F, Quehenberger O. The mouse *CCR2* gene is regulated by two promoters that are responsive to plasma cholesterol and peroxisome proliferator-activated receptor gamma ligands. Biochem Biophys Res Commun 2005;332:188–93.
[17] Weisberg SP, Hunter D, Huber R, Lemieux J, Slaymaker S, Vaddi K, et al. CCR2 modulates inflammatory and metabolic effects of high-fat feeding. J Clin Invest 2006;116:115–24.
[18] Kanda H, Tateya S, Tamori Y, Kotani K, Hiasa K, Kitazawa R, et al. MCP-1 contributes to macrophage infiltration into adipose tissue, insulin resistance, and hepatic steatosis in obesity. J Clin Invest 2006;116:1494–505.
[19] Kamei N, Tobe K, Suzuki R, Ohsugi M, Watanabe T, Kubota N, et al. Overexpression of monocyte chemoattractant protein-1 in adipose tissues causes macrophage recruitment and insulin resistance. J Biol Chem 2006;281:26602–14.
[20] Nesto RW, Bell D, Bonow RO, Fonseca V, Grundy SM, Horton ES, et al. Thiazolidinedione use, fluid retention, and congestive heart failure: a consensus statement from the American Heart Association and American Diabetes Association, October 7, 2003. Circulation 2003;108:2941–8.
[21] Guri AJ, Hontecillas R, Si H, Liu D, Bassaganya-Riera J. Dietary abscisic acid ameliorates glucose tolerance and obesity-related inflammation in db/db mice fed high-fat diets. Clin Nutr 2006 10.1016/j.clnu.2006.07.008.
[22] Akiyama TE, Sakai S, Lambert G, Nicol CJ, Matsusue K, Pimprale S, et al. Conditional disruption of the peroxisome proliferator-activated receptor gamma gene in mice results in lowered expression of ABCA1, ABCG1, and apoE in macrophages and reduced cholesterol efflux. Mol Cell Biol 2002;22:2607–19.
[23] Bassaganya-Riera J, Reynolds K, Martino-Catt S, Cui Y, Hennighausen L, Gonzalez F, et al. Activation of PPAR gamma and delta by conjugated linoleic acid mediates protection from experimental inflammatory bowel disease. Gastroenterology 2004;127:777–91.
[24] Kutlu B, Darville MI, Cardozo AK, Eizirik DL. Molecular regulation of monocyte chemoattractant protein-1 expression in pancreatic beta-cells. Diabetes 2003;52:348–55.
[25] Mokdad AH, Bowman BA, Ford ES, Vinicor F, Marks JS, Koplan JP. The continuing epidemics of obesity and diabetes in the United States. JAMA 2001;286:1195–200.
[26] Arner P. Regional adipocity in man. J Endocrinol 1997;155:191–2.
[27] Holness MJ, Bulmer K, Smith ND, Sugden MC. Investigation of potential mechanisms regulating protein expression of hepatic pyruvate dehydrogenase kinase isoforms 2 and 4 by fatty acids and thyroid hormone. Biochem J 2003;369:687–95.
[28] Boden G. Fatty acid-induced inflammation and insulin resistance in skeletal muscle and liver. Curr Diab Rep 2006;6:177–81.
[29] Shoelson SE, Lee J, Goldfine AB. Inflammation and insulin resistance. J Clin Invest 2006;116:1793–801.
[30] Lin HH, Faunce DE, Stacey M, Terajewicz A, Nakamura T, Zhang-Hoover J, et al. The macrophage F4/80 receptor is required for the induction of antigen-specific efferent regulatory T cells in peripheral tolerance. J Exp Med 2005;201:1615–25.
[31] Charriere G, Cousin B, Arnaud E, Andre M, Bacou F, Penicaud L, et al. Preadipocyte conversion to macrophage. Evidence of plasticity. J Biol Chem 2003;278:9850–5.
[32] Nibbering PH, Leijh PC, van Furth R. Quantitative immunocytochemical characterization of mononuclear phagocytes: I. Monoblasts, promonocytes, monocytes, and peritoneal and alveolar macrophages. Cell Immunol 1987;105:374–85.
[33] Phillips RJ, Lutz M, Premack B. Differential signaling mechanisms regulate expression of CC chemokine receptor-2 during monocyte maturation. J Inflamm (Lond) 2005;2:14.
[34] Tanaka T, Fukunaga Y, Itoh H, Doi K, Yamashita J, Chun TH, et al. Therapeutic potential of thiazolidinediones in activation of peroxisome proliferator-activated receptor gamma for monocyte recruitment and endothelial regeneration. Eur J Pharmacol 2005;508:255–65.
[35] Tsuchida A, Yamauchi T, Takekawa S, Hada Y, Ito Y, Maki T, et al. Peroxisome proliferator-activated receptor (PPAR)alpha activation increases adiponectin receptors and reduces obesity-related inflammation in adipose tissue: comparison of activation of PPARalpha, PPARgamma, and their combination. Diabetes 2005;54:3358–70.
[36] Pascual G, Fong AL, Ogawa S, Gamliel A, Li AC, Perissi V, et al. A SUMOylation-dependent pathway mediates transrepression of inflammatory response genes by PPAR-gamma. Nature 2005;437:759–63.
[37] Hevener AL, He W, Barak Y, Le J, Bandyopadhyay G, Olson P, et al. Muscle-specific PPARγ deletion causes insulin resistance. Nat Med 2003;9:1491–7.
[38] He W, Barak Y, Hevener A, Olson P, Liao D, Le J, et al. Adipose-specific peroxisome proliferator-activated receptor gamma knockout causes insulin resistance in fat and liver but not in muscle. Proc Natl Acad Sci U S A 2003;100:15712–7.